Supporting Information

0.1 Density of States Functions

We show how our dynamic programming method is used to compute the density of states, illustrating with a single helix. The information we need in dynamic programming is i, a particular level of our sequence, k, the number of consecutive coils starting at level i (going upward), and l the number of consecutive coils starting at level $i-1$ (going upward). The triple (i, k, l) is called a *state* of our helix. For example, Figure 4 of the manuscript shows the state $(4, 2, 0)$ of a 5 unit chain. A density of states function (DSF) is calculated for every state (i, k, l) by updating DSFs from the previous level $i - 1$. The DSF, $f(i, k, l)$, is updated differently depending on k and l. If $k > 0$ and $l = 0$, then level i is the start of consecutive coils and we update the chain's conformational count. If $k > 0$ and $l > 0$ then level i is somewhere in the middle of a string of coils and we don't update the density of states since we only update the chain's conformational count at the beginning of a tail or strand coil when we have information of a complete coil. Otherwise, level i is a helix (i.e. $k = 0$) and we update the number of hydrogen bonds and hydrophobic contacts in the chain. Figure 1 shows examples of states with these different cases.

A DSF g can be illustrated as a table like the following:

	0	1	2
0	71	18	3

Here the the top row represents the possible number of hydrophobic contacts and the left most column represents the number of hydrogen bonds. Here we have $g(0, 0) = 71$, $g(0, 1) = 18$, $g(0, 2) = 3$, and $g(N_{hb}, N_{\phi}) = 0$ for all other N_{hb}, N_{ϕ} pairs. This is the DSF for a single coil unit c. There is no hydrogen bonds and the maximum number of hydrophobic interactions is 2. For the simplicity of presentation, we first define some operators on DSFs that will be used later to describe the update rules.

Definition 1. The *sum* of two DSFs g and g', noted $g \oplus g'$, is another DSF defined as the point-wise addition:

$$(g \oplus g')(h, H) = g(h, H) + g'(h, H)$$

The $\oplus$ operator is used to combine the DSFs of two sub-cases in our algorithm. For example, here is another DSF g' which accounts for a single helix unit because the only possible configuration is to form a helical turn where there is exactly one hydrogen bond and one hydrophobic interaction:

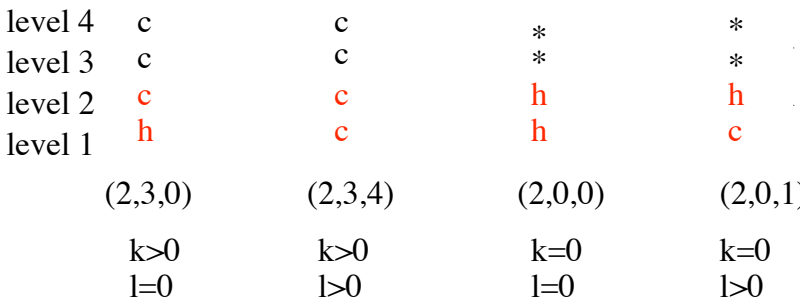

Figure 1: Conformation counts are updated only at the start of consecutive coils. This is the case when $k > 0$ and $l = 0$ as in state $(2, 3, 0)$. The case where $k > 0$ and $l > 0$ occurs when level i is in the middle of consecutive coils, as in state $(2, 3, 4)$. The state $(2, 0, 0)$ results in the addition of 3 hydrogen bonds and hydrophobic contacts, and the state $(2, 0, 1)$ results in the additon of a single hydrogen bond and hydrophobic contact.

	1
1	1

Then their sum $g'' = g \oplus g'$ is:

	0	1	2
0	71	18	3
1	0	1	0

which accounts for the total density of states of the two sequences `h` and `c`.

Similarly, we define convolution for computing the DSF of a longer sequence from the DSFs of two subsequences.

Definition 2. The *convolution* of two DSFs g and g', noted $g \otimes g'$, is another DSF defined as follows:

$$(g \otimes g')(h, H) = \sum_{i=0}^{h} \sum_{k=0}^{H} g(h - i, H - k) \cdot g'(i, k)$$

These operations are used, for example, to compute the DSF for the state $(3, 0, 0)$ from the *preceding states* $(2, 0, 1)$ and $(2, 0, 0)$ (see Figure 2). A state (i, k, l) always has two preceding states $(i - 1, l, l - 1)$ and $(i - 1, l, 0)$ corresponding to whether level $i - 2$ is `c` or `h` respectively. Here k is replaced by l because we are at level $i - 1$. The result of taking the convolution of the sum of the preceding states by a DSF in Figure 2 is to update the number of hydrogen bonds and hydrophobic contacts.

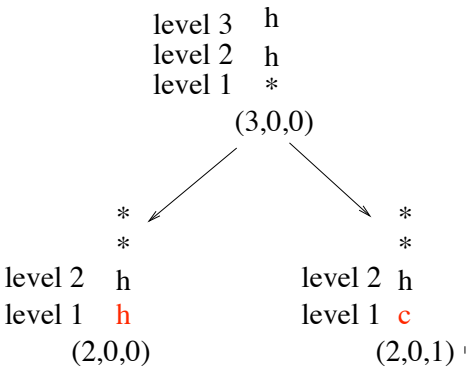

$$f(3,0,0) = (f(2,0,0) \oplus f(2,0,1)) \otimes \begin{array}{c|c} & 3 \\ \hline 3 & 1 \end{array}$$

Figure 2: The calculuation of the DSF, $f(3,0,0)$, involves the sum of the DSF for preceding states $(2,0,0)$ and $(2,0,1)$. Also there is the addition of three new hydrogen bonds and hydrophobic contacts achieved by convoluting with the DSF shown on the right of the equation.

0.2 An Example

We illustrate the inductive process of dynamic programming by calculating the density of states function for the four 2 level 1-helix sequences:

$$\begin{array}{cccc} \mathtt{h} & \mathtt{c} & \mathtt{h} & \mathtt{c} \\ \mathtt{h}, & \mathtt{h}, & \mathtt{c}, & \mathtt{c} \end{array}.$$

Let $f(i,k,l)$ be the density of states function for state (i,k,l).

Step 1: Compute $f(1,k,l)$ (base-case)

$f(1,0,0)$ is the DSF for having h in level 1 (i.e. having zero consecutive c at level 1). $f(1,1,0)$ is the DSF for having c in level 1 and h in level 2 . Finally, $f(1,2,0)$ is the DSF for having c in level 1 and in level 2 . All other level one DSF are zero.

$$\mathtt{h} \longleftrightarrow f(1,0,0) = \begin{array}{c|c} & 1 \\ \hline 1 & 1 \end{array}$$

$$\mathtt{c} \longleftrightarrow f(1,1,0) = \begin{array}{c|c|c|c} & 0 & 1 & 2 \\ \hline 0 & 71 & 18 & 3 \\ 1 & 0 & 1 & 0 \end{array}$$

$$\begin{matrix}\mathtt{c}\\ \mathtt{c}\end{matrix} \longleftrightarrow f(1,2,0) = \begin{array}{c|c|c|c|c|c} & 0 & 1 & 2 & 3 & 4 \\ \hline 0 & 9246 & 5512 & 2154 & 192 & 1 \end{array}$$

Step 2: Compute $f(2,k,l)$ (inductive-case)

Dynamic programming computes the $f(i,k,l)$ bottom up so we use our knowledge of the DSF for level $i = 1$ to compute the DSF for level $i = 2$. The state $(2,0,0)$ has non-zero preceding state $(1,0,0)$ (the second preceding state $(1,0,1)$ is zero by convention).

$$\begin{matrix}\mathtt{h}\\ \mathtt{h}\end{matrix} \longleftrightarrow f(2,0,0) = \Big(f(1,0,0) \oplus f(1,0,1)\Big) \otimes \mathbb{T}_{(3,3)}\overline{1}$$

Here $\mathbb{T}_{(3,3)}$ is the energy translation between levels 1 and 2. We are adding three hydrogen bonds and three hydrophobic bonds when we add a helical turn to a pre-existing helical turn. There is no conformational entropy contribution when adding a helical turn, hence the identity DSF $\overline{1}$. We have,

$$f(2,0,0) = \begin{array}{c|c} & 1 \\ \hline 1 & 1 \end{array} \otimes \begin{array}{c|c} & 3 \\ \hline 3 & 1 \end{array} = \begin{array}{c|c} & 4 \\ \hline 4 & 1 \end{array}$$

Similarly we have,

$$\begin{matrix}\mathtt{h}\\ \mathtt{c}\end{matrix} \longleftrightarrow f(2,0,1) = \Big(f(1,1,0) \oplus f(1,1,1)\Big) \otimes \mathbb{T}_{(1,1)}\overline{1}$$

$$= \begin{array}{c|c|c|c} & 0 & 1 & 2 \\ \hline 0 & 71 & 18 & 3 \end{array} \otimes \begin{array}{c|c} & 1 \\ \hline 1 & 1 \end{array}$$

$$= \begin{array}{c|c|c|c} & 1 & 2 & 3 \\ \hline 1 & 71 & 18 & 3 \end{array}$$

and,

$$\begin{matrix}\mathtt{c}\\ \mathtt{h}\end{matrix} \longleftrightarrow f(2,1,0) = \Big(f(1,0,0) \oplus f(1,0,1)\Big) \otimes \mathbb{T}_{(0,0)}tail(1)$$

$$= \begin{array}{c|c} & 1 \\ \hline 1 & 1 \end{array} \otimes \begin{array}{c|c|c|c} & 0 & 1 & 2 \\ \hline 0 & 71 & 18 & 3 \end{array}$$

$$= \begin{array}{c|c|c|c} & 1 & 2 & 3 \\ \hline 1 & 71 & 18 & 3 \end{array}$$

and,

$$\begin{matrix} c \\ c \end{matrix} \longleftrightarrow f(2,1,2) = \Big(f(1,2,0) \oplus f(1,2,3)\Big) \otimes \mathbb{T}_{(0,0)}\overline{1}$$

$$= \begin{array}{c|c|c|c|c|c} & 0 & 1 & 2 & 3 & 4 \\ \hline 0 & 9246 & 5512 & 2154 & 192 & 1 \end{array} \otimes \begin{array}{c|c} & 0 \\ \hline 0 & 1 \end{array}$$

$$= \begin{array}{c|c|c|c|c|c} & 0 & 1 & 2 & 3 & 4 \\ \hline 0 & 9246 & 5512 & 2154 & 192 & 1 \end{array}$$

Here, *tail*(1) is the DSF for a length 1 tail.

Step 3: We find f, the total DSF by adding together all top level functions.

$$f = f(2,0,0) \oplus f(2,0,1) \oplus f(2,1,2) \oplus f(2,1,0)$$

$$= \begin{array}{c|c|c|c|c|c} & 0 & 1 & 2 & 3 & 4 \\ \hline 0 & 9246 & 5512 & 2154 & 192 & 1 \\ 1 & & 142 & 36 & 6 & \\ 4 & & & & & 1 \end{array}$$

0.3 Testing the Density of States for the Three-Helix Bundle

Our helix bundle model is subject to constraints $1 \sim 8$ from section 2. To understand the effect of these constraints on conformation counts we compared our density of states prediction with an exact density of states calculation without constraints $4 \sim 7$. Exact enumeration was carried out by exhaustively enumerating all possible conformations. Figure 3 shows that our model does a good job of estimating conformation counts even with constraints $4 \sim 7$ in place. We chose energies $\epsilon_{hb} = 0.6$ kcal/mol, $\epsilon_{\phi} = 0.47$ kcal/mol, consistent with experimental 3-helix bundle data (see section 4.2). Exact enumeration was performed starting from the native 3-helix conformation and as a result, near native conformations are counted first followed by more open conformations. Conformational counts for energies less than -5 kcal/mol were very stable after 200 cpu hours and the self avoiding walk spent its time completing very open, low energy, conformations. The good fit between theory and experiment suggests that constraints $4 \sim 7$ in our model don't affect near native density of states.

0.4 van't Hoff and Calorimetric Enthalpy

By definition, the calorimetric enthalpy, ΔH_{cal}, is obtained by integrating the area under the excess heat capacity curve from a temperature well below the unfolding

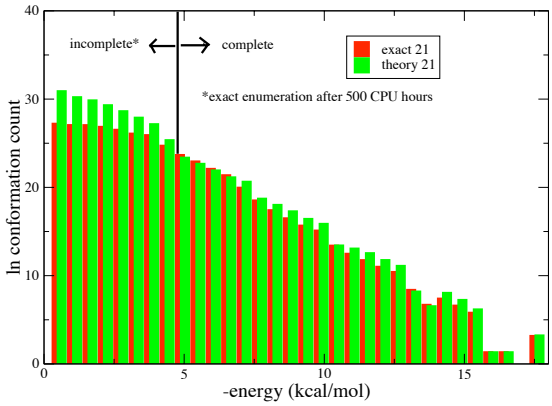

Figure 3: Theoretical density of states for 21 monomer 3-helix bundle versus exact enumeration. Exact enumeration is for a self avoiding walk in a cubic lattice with restrictions $1 \sim 3$ and 8 of section 2. Exact enumeration is incomplete for energies greater than -5 kcal/mol.

transition midpoint, T_0, to a temperature well above it, T_1:[1]

$$\Delta H_{cal} = \int_{T_0}^{T_1} C_P(T)\mathrm{d}T = \int_{T_0}^{T_1} \frac{\partial\langle H(T)\rangle}{\partial T}\mathrm{d}T = \langle H(T_1)\rangle - \langle H(T_0)\rangle = \langle H\rangle_D - \langle H\rangle_N. \tag{1}$$

Here the symbol $\langle \dots \rangle$ denotes Boltzmann averaging over the entire ensemble and

$$\langle H\rangle_N = \lim_{T_0\to 0}\langle H(T)\rangle$$

and

$$\langle H\rangle_D = \lim_{T_1\to \infty}\langle H(T)\rangle.$$

Equation 1 says the calorimetric enthalpy is equal to the difference between the average enthalpy of the denatured state $\langle H\rangle_D$ and the average enthalpy of the native state $\langle H\rangle_N$. By taking the limit as T_0 goes to zero and T_1 goes to infinity, we are capturing the entire transition process and not involving any empirical baseline subtraction. The result is a possible overestimation of calorimetric enthalpy compared to experimental values where T_0 and T_1 take finite values.

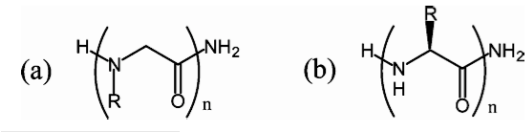

Figure 4: (a) Peptoid, or N-substituted glycine oligomer. (b) Peptide, for comparison.[7]

Several different definitions of van't Hoff enthalpy is currently used in the protein folding literature. However, when the thermodynamic cooperativity of a protein is high, the different definitions provide essentially the same restriction on enthalpy distribution.[2] Here we use the definition,

$$\Delta H_{vH} = 2T_{max}\sqrt{kC_{P,max}} \tag{2}$$

where T_{max} is the temperature at which the heat capacity attains its peak value, $C_{P,max}$, and k is the Boltzmann constant. The heat capacity is proportional to the variance (square of standard deviation σ_H) of the enthalpy,

$$C_P = \frac{\langle H^2(T)\rangle - \langle H(T)\rangle^2}{kT^2} = \frac{\sigma_H^2}{kT^2}. \tag{3}$$

It follows from equations 2 and 3 that the van't Hoff enthalpy is equal to two times the standard deviation of enthalpy at T_{max}:

$$\Delta H_{vH} = 2(\sigma_H)_{max}. \tag{4}$$

0.5 Peptoid Model

A peptoid is a N-substituted glycine polymer in which the side-chains are appended to the backbone nitrogen (see Figure 4). The polypeptoids relevant to this study, 15_Chi_FQ, 30_Chi_CN_FQ and 45_Chi_CN_FQ are synthesized, sequence-specific, 15mer, 30mer and 45mer polymers consisting of 15mer units chained together by disulfide and oxime linkages. Each peptoid bundle has a fluorescent probe, FP, and quencher probe, Q. The 15mer chiral sequence, 15_Chi_FQ has highly stable α-helix secondary structure despite its lack of hydrogen bond donors.[4,5] CD data indicates that acetonitrile does not break the helical secondary structure induced by the chirality of the side-chains. The acetonitrile only melts the long-range hydrophobic contacts of the peptoid.[7] Because of the stability of the helix formation, under ACN denaturation, the most unfolded state of a 2-helix

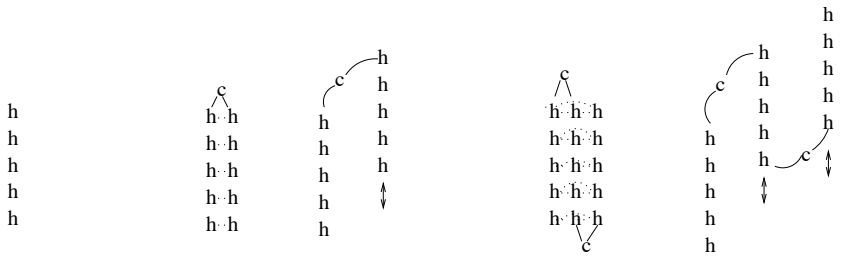

Figure 5: As a first approximation we model peptoid 1,2,3-helix bundles as having secondary structure intact in the unfolded state. Helix bundles either make a maximal number of inter-helical contacts or none at all. If no inter-helical contacts are made then the strands are allowed to move parallel one another.

bundle consists of the two helical cylinders tethered together. The increase in conformational entropy due to the breaking of inter-helical contacts is the driving force for denaturation.

Our model of a peptoid helix bundles follows the lattice and sequence model described above for protein helix bundles with certain modifications. As a first approximation, we do not allow helices the possibility of melting their secondary structure. Such a model is justified since ACN denaturation is believed to only effect tertiary interactions. A fully folded 1-helix bundle consists of 5 consecutive helix units (Figure 5). A fully folded 2-helix bundle consists of two sets of 5 consecutive helix units, tethered together by a single coil unit. The two strands can either form a maximal number of inter-helical contacts (folded state) or none at all. If the two strands make no inter-helical contacts then they must be parallel and travel opposite directions along the z axis as shown in Figure 5. A 3-helix peptoid consists of three sets of 5 consecutive helix units each tethered together by a single coil unit. Like, the 2-helix bundle, a 3-helix bundle may either have the maximal number of inter-helical contacts (folded state) or none at all. If the three strands make no inter-helical contacts then consecutive strands must be parallel and travel opposite directions along the z axis as shown in Figure 5.

As a refinement of the model, we allow the melting of intra-helical contacts. Our peptoid model is now similar to our protein model except for one modification. Whereas a 5 level, 2-helix bundle can form 10 consecutive helix units (as a 1-helix bundle), peptoids don't have this possibility because of the linkage unit in the middle of the chain which cannot form a helical turn. Similarly, in proteins, a 5 level, 3-helix bundle can form 15 consecutive helix units (as a 1-helix bundle), but peptoids have linkage units dividing the chain into thirds.

To make a FRET efficiency plot we defined the fluorescent probe, FP, and quencher, Q, of peptoids to be specific monomers in our peptoid model and measured their distance apart in the lattice for each conformation. For example, if FP and Q are on adjoining sites of our lattice then they would be distance $r = 1$ unit apart. In our model 1 lattice unit corresponds to 6 Angstroms. 2D-NMR and X-ray crystallographic studies of pentameric peptoids show that helices contain 3 residues per turn and have a pitch of roughly 6 Angstroms .[7] The distance r between the donor and quencher was related to the fluorescence Γ by the equation:

$$\Gamma(r) = \frac{31^6}{r^6 + 31^6}. \tag{5}$$

To match the experimental data we needed to make several ad hoc adjustments when computing the distance between donor and quencher. We took account of the dependence of helical pitch on ACN concentration by making the distance conversion from lattice units to Angstroms be a linearly increasing function of ACN concentration. Also we calibrated the distance between FP and Q for the folded states of our 2-helix and 3-helix to match the distance between donor and quencher of the 1-helix bundle (approximately 23 Angstroms) so the FRET efficiency of all peptoid bundles would be the same at O M ACN.

For each peptoid we computed the energy, E,

$$E = \epsilon_{hb} \cdot N_{hb} + \epsilon_{\phi} \cdot N_{\phi} + \epsilon_c \cdot N_c.$$

The first part of the energy consists of the stacking interaction energy of the chiral side chains, which we call ϵ_{hb}, times the number of stacking interactions, N_{hb}. The other terms of the energy are the same as for proteins in equation 1. As before, ϵ_{hb} and ϵ_{ϕ} are linear functions of ACN concentration of the form $a + b \cdot [D]$ for some fixed parameters a and b. Because ACN is a hydrophobic solvent that shouldn't effect the stacking interaction energy of the chiral side chains, we made ϵ_{hb} independent of ACN concentration.

Using dynamic programming we found the density of states and the average distance between FP and Q. We computed the FRET efficiency corresponding to the average distance between FP and Q for each energy level using equation 5. The average FRET efficiency is the weighted sum of the FRET efficiency for each energy level.

References

1. Privalov, P.; Khechinashivili, N. *J. Mol. Biol.*, **1974**, *86*, 665–684.

2. Chan, H. *Proteins: Structure Function and Genetics*, **2000**, *40*, 543–571.

3. Kirshenbaum, K.; Zuckermann, R.; Dill, K. *Curr. Opin. Struc.Bio.*, **1999**, *9*, 530–535.

4. Kirshenbaum, K.; Barron, A.; Goldsmith, R.; Armand, P.; Bradley, E.; Truong, K.; Dill, K.; Cohen, F.; Zuckermann, R. *Folding and Design*, **1997**, *2*(6), 369–375.

5. Kirshenbaum, K.; Barron, A. E.; Goldsmith, R. A.; Armand, P.; Bradley, E. K.; Truong, K. T. V.; Dill, K. A.; Cohen, F. E.; Zuchermann, R. N. *Proc. Natl. Acad. Sci.*, **1998**, *95*, 4303–4308.

6. Burkoth, T.; Beausoleil, E.; Kaur, S.; Tang, D.; Cohen, F.; Zuckermann, R. *Chemistry and Biology*, **2002**, *9*, 647–654.

7. Lee, B.-C.; Zuckermann, R. N.; Dill, K. A. *Journal of the American Chemical Society*, **2005**.